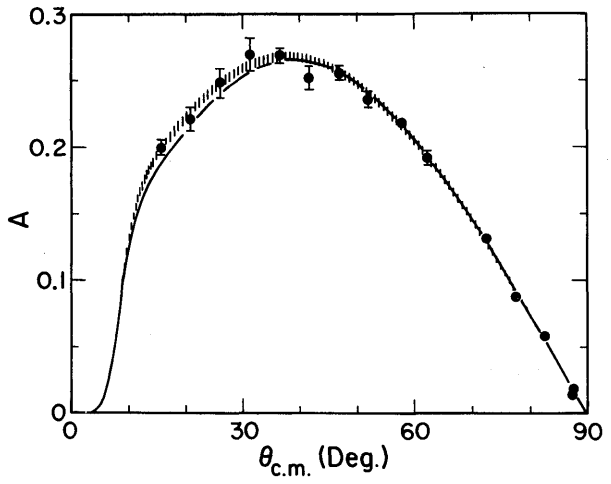

Figure 2. The analyzing power for p-p scattering at 180 MeV. The solid curve is Arndt's global phase shift solution SM86. The vertical bars represent Arndt's C200 single energy solution with error estimates.

background subtraction. This is done because of the preliminary stage of the analysis and also to illustrate the size of the background corrections. The normalization of the data is taken from the high energy polarimeter calibration as described above. The curve is the prediction of Arndt's SM86 global solution,[2] while the vertical bars represent the C200 single-energy solution with error estimates. The difference in the two curves can be traced to the $^1D_2$ phase shift parameter. These data should also further constrain the ε_2, $^3P_1$ and $^3F_2$ parameters.

1) H. Spinka, in Nuclear Physics with Stored, Cooled Beams, ed. P. Schwandt and H.O. Meyer, (AIP, New York, NY, 1985) p. 198

2) R.A. Arndt, J.S. Hyslop III, and L.D. Roper, Phys. Rev. D 35, 128 (1987).

3) G.F. Cox et al., Nucl. Phys. B4, 353 (1967).

4) See contributions to this report, p. 8.

5) 1985 IUCF Scientific and Technical Report, p. 125.

TENSOR POLARIZED DEUTERON CAPTURE BY THE HYDROGEN ISOTOPES

W.K. Pitts†, H.O. Meyer, L.C. Bland, J.D. Brown§, R.C. Byrd¶, M. Hugi††, H.J. Karwowski‡, P. Schwandt, A. Sinha‡‡, J. Sowinski, and I.J. van Heerden‡‡
Indiana University Cyclotron Facility, Bloomington, Indiana 47405

It is with great relief that we announce the end of E234, a measurement of the angular distribution of the cross section $\sigma(\theta)$, vector analyzing power A_y, and tensor analyzing power A_{yy} for the $^1H(\vec{d},\gamma)^3He$ and $^2H(\vec{d},\gamma)^4He$ reactions. Preliminary results have been reported at the Lake Louise conference[1] and the final results for the $^1H(d,\gamma)^3He$ reaction have been submitted to the Physical Review. The analysis of the $^2H(d,\gamma)^4He$ reaction is nearly complete, and these results will also soon be submitted for publication.

The interest in these reactions is due to the sensitivity of the tensor analyzing power to the D-state component of ^3He and ^4He. Since the D-state is mixed with the dominant S-state component by the tensor force, A_{yy} is linked to the tensor force in nuclei.[2] In the case of ^3He, a Faddeev calculation of the $^1H(d,\gamma)^3He$ reaction with the Reid soft-core potential showed that 95% of the tensor analyzing power A_{yy} was due to the D-state of ^3He.[3] A_{yy} vanished when the Malfliet-Tjon potential (which does not have a tensor

force) was used instead of the Reid soft-core potential. In a similar fashion A_{yy} for the $^2H(\vec{d},\gamma)^4He$ reaction should be sensitive to the D-state component of ^4He. This reaction proceeds predominantly through an E2 transition because of parity and isospin restrictions due to the presence of identical bosons in the entrance channel. The angular distribution then has a $\sin^2 2\theta$ shape. Since there are only eight amplitudes contributing to this reaction, a complete multipole decomposition can be carried out if all analyzing powers are measured. This has been done at $E_d \approx 10$ MeV by a group at the University of Wisconsin, and it was found that there were significant admixtures of other multipoles besides the E2.[4] Calculations by Tostevin[5] have succeeded in reproducing A_{yy} and the vector analyzing moment A_y from this data set, but not the spherical tensor power T_{20}. A possible cause of this behaviour is that T_{20}, and not A_{yy}, is sensitive to the highly distorted $^5S_2$ amplitude. A complete solution of this problem (including an umambiguous measure of the D-state effects) will probably not be found until complete four-body calculations are carried out.

Another interesting aspect of the $^2H(\vec{d},\gamma)^4He$ reaction is that the cross section at higher energies ($E_d \approx 400$ MeV) is dramatically different from that observed at lower energies. The angular distribution for $\sigma(\theta)$ is peaked at $\theta \approx 90°$ rather than at $\theta(45°)$. This behaviour has been observed (although with poor statistics) at several energies.[6,7] In fact, the original motivation for our study of the $^2H(\vec{d},\gamma)^4He$ reaction was to measure $\sigma(\theta)$ in an effort to understand the reaction mechanism. The deviation of $\sigma(90°)$ from zero should be a sensitive measure of the deviation from the expected reaction mechanism, since other multipoles or other components of the wavefunction (such as the D-state) will tend to fill the minimum.

2. The Experiment

Since the cross section for the $^2H(\vec{d},\gamma)^4He$ reaction is less than 2nb/sr, measurements of this reaction must be optimized to make efficient use of accelerator time. The performance of the apparatus must also be optimized to cleanly distinguish radiative capture events from the background of strong reactions. Another problem with such a low-rate experiment is that it is difficult to monitor the reaction during data acquisition and practically impossible to set up the electronics with the $^2H(\vec{d},\gamma)^4He$ reaction. Our approach was to use the $^1H(\vec{d},\gamma)^3He$ reaction for setting up the electronics and matching the gains in the detectors. Interspaced with the $^2H(\vec{d},\gamma)^4He$ data acquisition runs were additional $^1H(\vec{d},\gamma)^3He$ runs about every eight hours to check for gain shifts. For this purpose, nothing except the target would be changed. Our philosophy was that if the responses of the detectors to photons and ^3He nuclei from the $^1H(\vec{d},\gamma)^3He$ spectra were as expected, then the $^2H(\vec{d},\gamma)^4He$ data would be successfully acquired, also.

The incident deuteron beam readily generates neutrons at these energies, causing a large neutron induced background in the photon detectors due to such processes as neutron excitation of giant resonances or quasi-elastic scattering. A sodium iodide detector would be sensitive to practically all of the decay branches such as (n,n'p), (n,n'γ) or (n,n'α). At these energies it would be difficult to measure the analyzing powers of $^2H(\vec{d},\gamma)^4He$ by detecting only the photon in a large sodium iodide scintillation detector due to the combination of the small radiative capture cross section and the large neutron-induced background. Fortunately, both ^3He and ^4He have only

one particle-stable state, and so it is possible to measure the photon and the helium nucleus in coincidence. The photon detector can then have relatively poor resolution and still effectively identify radiative capture events. The photon detectors were eight large, lead-glass Cerenkov detectors which have been built for previous experiments at the IUCF.[8] These detectors have very good timing resolution (typically about 800 ps FWHM) and are insensitive to neutrons except through reactions such as $(n,n'\gamma)$.

The major problem associated with these coincidence measurements was that the helium nuclei are emitted at small angles from the beam axis. In this angular region there is a large flux of Coulomb scattered deuteron from carbon in the CH_2 or CD_2 targets. The detector was a three element plastic scintillator telescope with a very fast timing response (500 ps FWHM) which could operate in this high background environment without significant gain shifts. The problem was to reconcile the requirements of a small size (to reduce the singles rates) with the necessity of detecting all the coincident helium nuclei, while balancing the light output between the first two detector planes for ^{4}He nuclei from the $^2\vec{H}(d,\gamma)^4$He reaction. A third plane stops all the ^{3}He nuclei from the $^1\vec{H}(d,\gamma)^3$He reaction and also vetoes events due to minimum ionizing particles such as protons and deuterons. The design of the telescope was optimized using a Monte-Carlo simulation of the detector telescope that included the effects of energy loss and multiple scattering in the target as well as the non-linear light output responses. The correlation of pulse height in the first plane and the sum of all three planes was then used for charge identification. Once the charge of a particle was known its mass could be found from the time-of-flight spectrum. The timing properties of this detector were crucial, since it was necessary to isolate a $^2H(d,\gamma)^4$He event rate of several tens of events per hour in the recoil detector from a deuteron singles rate of 2 MHz. The triple time correlation between the helium detector, the pulsed beam of the cyclotron (driven at the RF frequency of 28.57 MHz), and the photon detectors was used to isolate the radiative capture events.

The apparatus is shown in Fig. 1. The photon detectors are labeled PB1L, PB2L, etc. and the two recoil telescopes are labeled H1L, H2L, etc. The apparatus was symmetric about the beam axis, so that the left-right asymmetry could be measured (for a given beam polarization) as well as the asymmetry between beams of different polarizations. Both asymmetries can

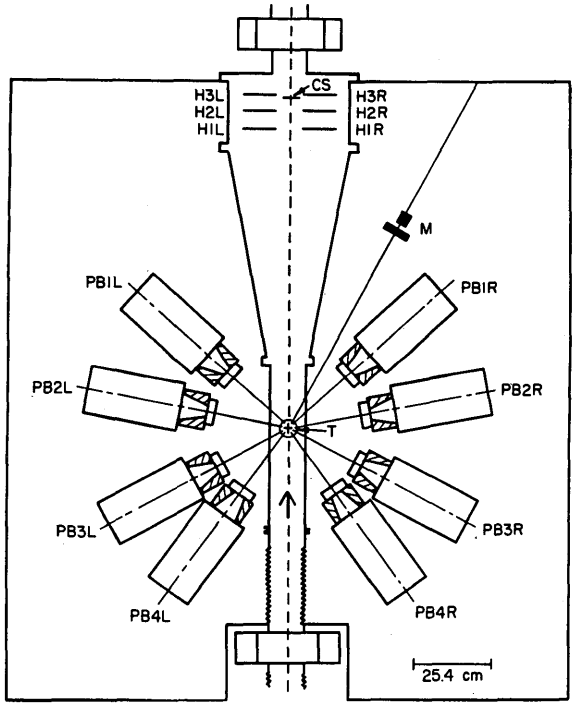

Figure 1. Experimental apparatus for E 234.

be used to calculate the analyzing powers, and some possible errors can be cancelled by taking averages between polarization states or lift-right asymmetries. Also shown in Fig. 1 is a movable scintillator (CS) between the two recoil telescopes. This scintillator was used in conjunction with a scintillator on the target ladder (T) to center the beam with respect to the two telescopes. By the time the beam envelope was adjusted to be in the 2 mm × 2mm holes of these scintillators it was necessarily of small divergence, and could then be adjusted to have a small halo. It was necessary to periodically monitor the deuterium content of the target due to loss of deuterium. A target thickness monitor (M) consisting of a plastic scintillator, active slit, and sodium iodide scintillator was used to monitor the CD_2 targets throughout the measurement.

The timing response of the Cerenkov detectors to 32 MeV photons from the $^1H(d,\gamma)^3He$ reaction is shown in Fig. 2. The large peak to the left of the photon peak is an artifact of the discriminator, which is cutting into a smooth neutron background. Note that even with a flight path of only 35 cm the timing resolution was still adequate to distinguish between photons and fast neutrons. Unfortunately the pulse height resolution is poor, since the Cerenkov process does not generate a large amount of light. The typical pulse height resolution was only about 40% for these 32 MeV photons.

The recoil telescope provided excellent particle identification. Figure 3 shows the measured responses for the helium isotopes with the CD_2 target. (The ^3He nuclei are from the $^2H(\vec{d},{}^3He\gamma)n$ reaction.) The predicted light output from the Monte-Carlo simulation was normalized to the measured ^3He responses, generating the gains and offsets. Notice that the timing resolution of 500 ps (FSHM) is sufficient to distinguish between the two isotopes. The pulse height resolution was typically 8% for the summed pulse height. Since there was a large flux of beam energy deuterons, the pulse heights of 10% of the radiative capture events were shifted by the pulse height of deuteron. This did not cause any problems with the particle identification, since the additional light from the charge Z=1 particle was significantly less than the light from the helium nucleus.

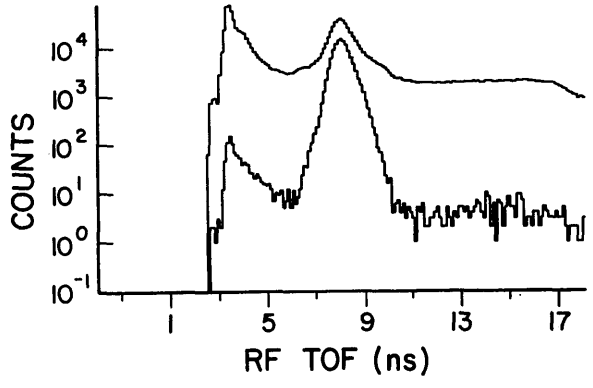

Figure 2. Timing response of the photon detectors for 32 MeV photons, with and without the sorting conditions for radiative capture.

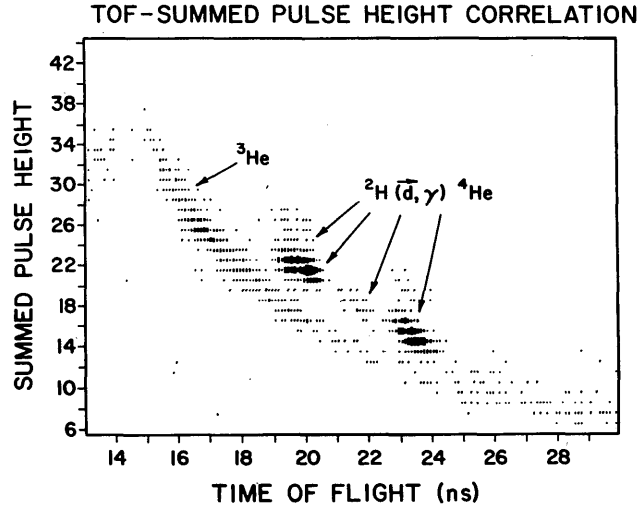

Figure 3. Time of flight-pulse height correlation for the $^2H(\vec{d},\gamma)^4He$ reaction. Gated by photon time of flight and pulse height, as well as pulse height in the first plane of the telescope.

The final time-of-flight spectra for the $^2H(\vec{d},\gamma)^4He$ reaction (with all cuts) is shown in Fig. 4. The background under the peak is due to the $^2H(\vec{d},{}^3He)n$ reaction, and this contribution was subtracted from the cross section. The corresponding spectrum for the $^1H(d,\gamma)^3He$ reaction had practically no background; the contribution from the carbon in the CH_2 target was measured with a pure carbon target and then subtracted from the peak sum. The error budget for the $^2H(\vec{d},\gamma)^4He$ cross section is shown in Table I, and the error budget for the $^1H(\vec{d},\gamma)^3He$ cross section is shown in Table II. The plots of $\sigma(\theta)$ include these systematic uncertainties in addition to the statistical errors.

The tensor polarization of the beam was cycled through the spin states "unpolarized", "tensor minus", and "tensor plus" with 60 seconds for each state. (The vector polarization could not be reversed with fast spin-flip since stray magnetic fields ruined the weak-field states.) The vector analyzing power A_y was calculated from the left-right asymmetry and the tensor analyzing power was calculated from the spin-flip asymmetry. Averaging the analyzing powers between the spin states or sides reduced some possible systematic errors associated with a typical measurement of the polarization. A systematic uncertainty of 5% from the polarimeter calibration is not shown.

3. Results of the $^2H(d,q)^4He$ Measurement

The preliminary results of this measurement are shown in Fig. 5. These data were fit with Legendre functions, since the coefficients of these functions can be related to sums of amplitudes. The fit to A_{yy} indicated the need for other multipoles (or possible D-state effects) is also indicated by the non-zero cross section at 90°. It is clear, however, from the shape of the angular distribution that the reaction at

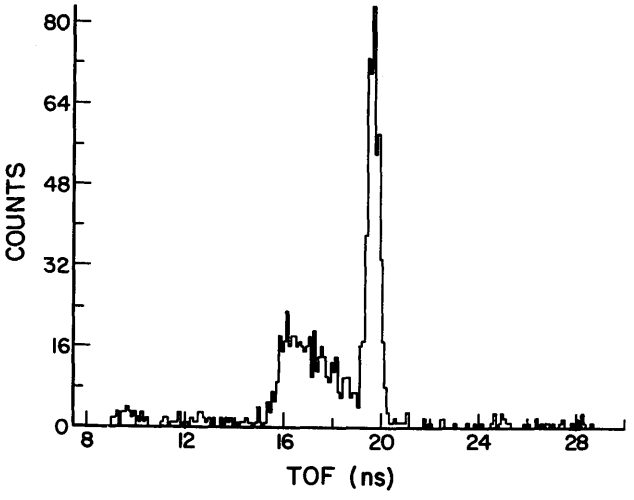

Figure 4. One of the final TOF spectra for the $^2H(d,\gamma)^4He$ reaction, with full radiative capture conditions. Accidentals have not yet been subtracted.

Table I. Systematic error budget for the $^1H(d,\gamma)^3He$ cross section

Error Source	Uncertainty(%)
TDC shifts	0.75
Multiple Scattering	1.0
Photon detector efficiency	2.0
Photon conversion in collimator	1.0
RF Sorting cut	0.5
Reaction effects in telescope	1.0
Carbon	0.25
Geometric effects: translations	2.3
Geometric effects: tilt	2.5
Errors added in quadrature	4.3

Table II. Systematic error budget for the $^2H(d,\gamma)^4He$ cross section

Error Source	Uncertainty (%)
TDC shifts	0.75
Photon detector efficiency	2.0
Photon conversion in collimator	3.0
RF sorting cut	1.0
Reaction effects in telescope	1.0
$^2H(d,{}^3He\gamma)n$ subtraction: 90,99°	5.0
$^2H(d,{}^3He\gamma)n$ subtraction: other angles	3.0
Deuterium content	4.0
Geometric effects: tilt	2.5
Geometric effects: translation	2.3
Errors added in quadrature (90°)	7.8
Errors added in quadrature (other angles)	6.7

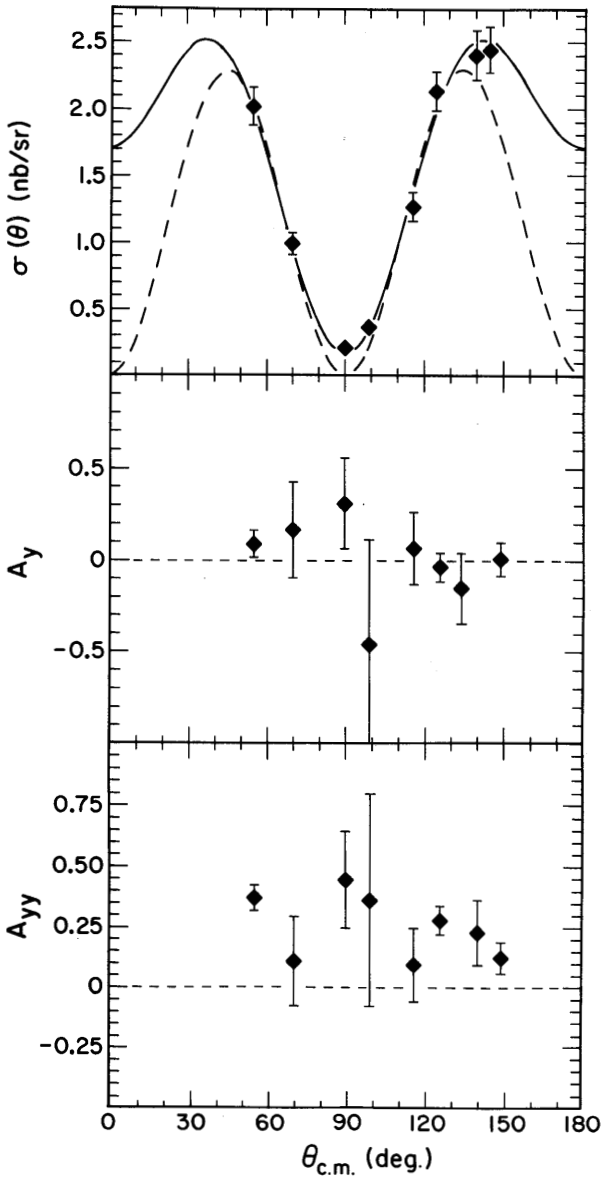

Figure 5. Preliminary results for the $^2H(\vec{d},\gamma)^7He$ reaction. The solid curve is a fit to $\sigma(\theta)$; the dashed curve for $\sigma(\theta)$ is a $\sin^2 2\theta$ curve normalized to the 55° data point.

this energy is still E2-dominated. The additional multipole is perhaps the E1 multipole, since the restriction to the E1 multipole (from isospin conservation) is strictly valid only in the long-wavelength limit. (It should be pointed out that we cannot experimentally distinguish E1 effects from M2 effects with this data set.) A significant amount of both E1 and M2 strength was revealed in the multipole decomposition of this reaction at Wisconsin (E_d = 10 MeV); as the energy is increased the long-wavelength approximation becomes progressively worse. Extraction of any information concerning D-state effects from this data will be problematic, since there are no reliable calculations of this reaction at our energy (E_d = 95 MeV). The best available calculation is that of Tostevin,[5] who found that an extrapolation to our energy gave a negative tensor analyzing power.[10] Plane waves were used for the entrance channel since

there is a near-total lack of information on the entrance channel and its distortion at E_d = 95 MeV. While this study is unlikely to yield any new knowledge on the D-state component of ^{4}He at this time, we should be able to determine the extent to which the reaction is not an E2 transition. This determination will then shed some light on the reaction mechanism of this reaction, and serve as a guide in planning studies of this reaction at other energies.

4. Results of the ^{1}H(d,γ)^{3}He Measurement

Our data for this reaction are shown in Fig. 6, along with the predictions of a PWBA model used to interpret the data.[11] This model used a Faddeev calculation of the ^{3}He projected into proton and deuteron channels for the ^{3}He wavefunction; plane waves were used for the entrance channel. In this calculation the D-state component of ^{3}He is parameterized by the asymptotic D-S normalization ratio η, and η was generated by matching the Faddeev wavefunction to the asymptotic Hankel wavefunction at 6 fm. This particular value of η, -0.029, gave an acceptable fit to both our data at E_d = 95 MeV and other measurements of A_{yy} at E_d = 29.8 MeV. Since the three-body system can be solved exactly, one would like to compare these data to a full Faddeev treatment which generates both the continuum and bound state wavefunctions in a self-consistent manner. This has been done at E_d = 29.2 MeV, where it was found that most of the tensor analyzing power was due to ^{3}He configurations with a correlated pair in a state of orbital angular momentum ℓ = 1 orbited by the third nucleon in a state with orgital angular momentum ℓ = 1 relative to the pair.[3] This configuration is orthogonal to those used in the projected wavefunction, which only allows real deuterons of orbital angular momentum ℓ = 0 or ℓ = 2. Resolution of this

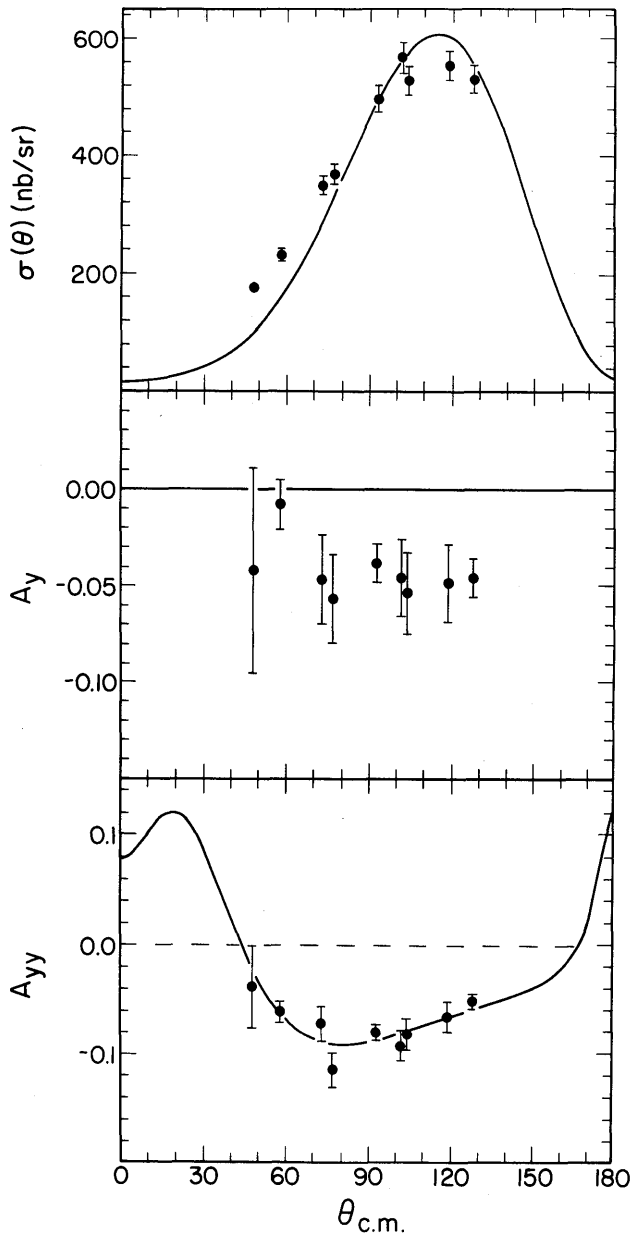

Figure 6. Final results for the ^{1}H(d,γ)^{3}He reaction. The solid curves are the PWBA calculation of Arriaga and Santos, which is described in the text.

controversy must wait for further theoretical efforts. Our results for this reaction have been submitted to Physical Review.

The calculations and insight of A. Arriaga, F.D. Santos, and J.A. Tostevin are gratefully acknowledged. The assistance and cooperation of P.T. Debevec, S. Lebrun, and A.M. Nathan of the University

of Illinois with the tests of the photon detectors is very much appreciated. Discussions with S.W. Wissink were always valuable. C.S. Yang, and V.R. Cupps contributed to the early stages of this work.

Present address:

†Univ. of Illinois Urbana-Champaign, Urbana, IL 60801

§Princeton University, Princeton, NJ 08544

¶Los Alamos National Lab, Los Alamos, NM 87545

††Fluehwiesenweg 5, CH-8116, Wurenlos, Switzerland

‡University of North Carolina, Chapel Hill, NC 27514

+University of Bonn, Bonn, FRG

++Univ. ov the Western Cape, Belleville, South Africa

1) W.K. Pitts, Proceedings of the Second Conference on the Intersections Between Particle and Nuclear Physics, Lake Louise, Canada, 1986, ed. D.F. Geesaman, AIP Conference Proceedings 150, New York (1986).

2) T.E.O. Ericson and M. Rosa-Clot, Ann. Rev. Nucl. Part. Sci. 35, 271 (1985).

3) J. Jourdan, M. Baumgartner, S. Burzyndki, P. Egelhof, A. Klein, M.A. Pickar, G.R. Plattner, W.D. Ramsey, H.W. Roser, I. Sick, and J. Torre, Phys. Lett 162B, 269 (1986); J. Jourdan, M. Baumgartner, S. Burzynski, P. Egelhof, R. Henneck, A. Klein, M.A. Pickar, G.R. Plattner, W.D. Ramsey, H.W. Roser, I. Sick, and J. Torre, Nucl Phys. A453, 220 (1986);

4) S. Mellema, T.R. Wang, and W. Haeberli, Phys. Rev. C 34, 2043 (1986).

5) J.A. Tostevin, Phys. Rev. C 34, 1497 (1986).

6) J. Arends, J. Eyink, T. Hegerath, H. Hartmann, B. Mecking, G. Noldeke, and H. Rost, Phys. Lett. 62B, 411 (1976).

7) B.H. Silverman, A. Boudard, W.J. Briscoe, G. Bruge, P. Couvert, L. Farvaque, D.H. Fitgerald, C. Glashausser, J.-C. Lugol, and B.M.K. Nefkens, Phys. Rev. C 29, 35 (1984).

8) M.A. Pickar, Ph.D. Thesis, Indiana University (1982).

9) R.G. Seyler and J.R. Weller, Phys. Rev. C 31, 1952 (1985).

10) J.A. Tostevin, private communication

11) A. Arriaga and F.D. Santos, Phys. Rev. C 29, 1945 (1984).

STATUS OF THE 3-BODY $\vec{d}$+p BREAKUP EXPERIMENT

D.A. Low, C. Olmer, A. Opper, P. Schwandt, K.A. Solberg, E.J. Stephenson, and S.W. Wissink
Indiana University Cyclotron Facility Bloomington, Indiana 47405

Recently, there has been considerable interest in the off-shell components of the fundamental nucleon-nucleon interaction. Specifically, predictions of current models and parameterizations yield similar on-shell (asymptotic) features, but differ in their off-shell (interior) behavior. Many experiments have examined low-energy 3-body observables in various geometries intended to enhance off-shell effects. Unfortunatly, those experiments have suffered from either large Coulomb effects, or in the case of neutron experiments, insufficient precision. The need to utilize energies which would limit the importance of the Coulomb contribution led to the suggestion that experiments should be carried out which utilize energies of greater than 40 MeV per nucleon. We chose to examine the d+p breakup system at E_d=95 MeV in a geometry which necessitates a large momentum change for each of the nucleons. The small relative distances required in such a kinematic condition may enhance off-shell effects. In addition, we want the protons to